Effective antiplane shear wave speed in 2D periodic piezoelectric crystals

A.A. Kutsenko[a], A.L. Shuvalov[a], A.N. Norris[b,*]

[a] *Institut de Mécanique et d'Ingénierie de Bordeaux, Université de Bordeaux, UMR CNRS 5469, Talence 33405, France*
[b] *Mechanical and Aerospace Engineering, Rutgers University, Piscataway, NJ 08854-8058, USA*

Abstract

Effective anti-plane quasistatic moduli for 2D piezoelectric phononic crystals of arbitrary anisotropy are formulated analytically using the plane-wave expansion (PWE) method and the recently proposed monodromy-matrix (MM) method. The latter approach employs Fourier series in one dimension with direct numerical integration along the other direction. As a result, the MM method converges much quicker to the exact moduli in comparison with the PWE as the number of Fourier coefficients increases.

1. Introduction

There is considerable interest in periodic structures with some or all of the constituents having piezoelectric properties, e.g. for electromechanical coupling in phononic crystals (PCs). Design of PCs for application requires very accurate prediction of homogenized properties based on knowledge of the constituent parameters. Several techniques, exact and approximate, have been proposed for estimating the effective properties of periodic piezoelectric composites. For instance, [1] analyzed binary piezoelectric composites with unidirectional fibres using an approximation scheme, "equivalent homogeneity". Micromechanical models appropriate to specific inclusion shapes have been used to predict effective properties, e.g. spheres and ellipsoids [2] or circular and square cylinders [3]. Dynamical solutions for periodic piezoelectric composites were obtained in [4] using Bloch expansion techniques, and macroscopic effective coefficients were obtained in the quasistatic limit. Two-phase parallel fiber-reinforced periodic piezoelectric composite were considered in [5] using the asymptotic homogenization method (AHM, see also [6]) and the eigenfunction expansion-variational method (EEVM, see also [7]). Finite element methods have been employed to compute homogenized properties, e.g. [8] evaluated effective coefficients for square and hexagonal arrangements of piezoelectric cylindrical fiber composites. An alternative numerical homogenization method based on FEM and calculated wave speeds is described in [9]. The anti-plane or SH (shear horizontal) case allows the use of complex variable techniques, as in [10, 11] which considered, respectively, square and doubly periodic arrangements of circular cylinders embedded in a homogeneous medium. Exact complex-variable techniques and approximations were also used in [12] to estimate effective anti-plane properties of piezoelectric fibrous composites. Reviews of the effective properties of piezoelectric composites and methods for their estimation can be found in [13, 14].

Despite the variety of homogenization schemes that have been considered there appears to have been little if any application of the Plane Wave Expansion (PWE) method. The PWE technique is widely used for calculating dispersion curves of acoustic and electromagnetic waves in PCs. PWE is based on Fourier expansions; in the zero frequency limit the method provides a simple and versatile numerical approach for calculating the quasi-static wave speeds, from which the effective properties can be determined, e.g. see [15] for applications in acoustics. While the PWE method is robust and simple to implement, it can become

*Corresponding author
Email addresses: aak@nxt.ru (A.A. Kutsenko), a.shuvalov@i2m.u-bordeaux1.fr (A.L. Shuvalov), norris@rutgers.edu (A.N. Norris)

numerically expensive especially when dealing with large contrast in material properties. The recently proposed Monodromy Matrix (MM) approach [16, 17] significantly reduces this problem by avoiding Fourier expansion in one of the coordinates, leading to much faster convergence than PWE.

The purpose of the present paper is to extend both the PWE and MM methods to provide accurate schemes for calculating effective wave speeds in piezoelectric PCs. For clarity we consider the case of SH waves in two-dimensional (2D) phononic crystals. The PWE is presented here in a compact form (see eq. (17)) suitable for numerical implementation. The main thrust of the paper is concerned with the MM approach. The motivation for advocating this method as an alternative to the more conventional PWE technique is that the MM method is numerically more efficient and provides faster convergence. Comparison of MM and PWE calculations provided here confirms the significantly better efficiency of the MM method.

The paper is organised as follows. The governing equations are introduced in §2. The PWE and MM methods are explained in §3 and §4, respectively. It is shown in §5 that both approaches yield the closed form expressions for the case of 1D periodicity. Procedures for numerical implementation of the PWE and MM methods are described in §6 and example computations and comparisons are provided in §7. Conclusions are given in §8.

2. Background: Equations of piezoelectricity

Consider a 2D periodic piezoelectric phononic crystal which is uniform in the out-of-plane direction $x_3 = X_3$, where $\{x_1, x_2, x_3\}$ are orthogonal coordinates and $\{X_1, X_2, X_3\}$ are the crystalline axes. Within the quasistatic approximation, the governing equations of piezoacoustics for the out-of-plane SH wave are

$$\begin{gathered}\sigma_{3i} = c_{3ij3}\nabla_j u + e_{k3i}\nabla_k\varphi,\ D_i = -\varepsilon_{ij}\nabla_j\varphi + e_{ik3}\nabla_k u;\\ \nabla_i\sigma_{3i} = -\rho\omega^2,\ \nabla_i D_i = 0\end{gathered} \tag{1}$$

where σ_{ij} is stress, u is SH displacement, D_i is electric displacement, φ is the electric potential, c_{ijkl}, e_{ijk} and ε_{ij} are the tensors of elastic, piezoelectric and dielectric permittivity coefficients, ρ is the density, ω is the wave frequency, $\nabla_i \equiv \partial/\partial x_i$, $i, j, k = 1, 2$ and the summation over repeated indices is adopted. Equations (1) can be rewritten in the form

$$\begin{pmatrix}\boldsymbol{\nabla}^\top\mathbf{a}\boldsymbol{\nabla} & \boldsymbol{\nabla}^\top\mathbf{b}^\top\boldsymbol{\nabla}\\ \boldsymbol{\nabla}^\top\mathbf{b}\boldsymbol{\nabla} & \boldsymbol{\nabla}^\top\mathbf{c}\boldsymbol{\nabla}\end{pmatrix}\begin{pmatrix}u\\ \varphi\end{pmatrix} = -\omega^2\boldsymbol{\rho}\begin{pmatrix}u\\ \varphi\end{pmatrix}\ \text{with}\ \boldsymbol{\rho} = \begin{pmatrix}\rho & 0\\ 0 & 0\end{pmatrix}, \tag{2}$$

where $^\top$ means transpose and $\mathbf{a}$, $\mathbf{b}$ and $\mathbf{c}$ are 2×2 matrices of shear, piezoelectric and dielectric coefficients with the components

$$a_{ij} = c_{3ij3},\ b_{ij} = e_{i3j},\ c_{ij} = -\varepsilon_{ij},\ i, j = 1, 2. \tag{3}$$

Alternatively, eqs. (1) can be recast into the form

$$\begin{gathered}\boldsymbol{\eta}' = \mathbf{Q}\boldsymbol{\eta}\ \text{ with }\ ' \equiv \nabla_1,\ \boldsymbol{\eta} = \big(u, \varphi, \sigma_{31}, D_1\big)^\top,\\ \mathbf{Q} = \begin{pmatrix}\mathbf{h}\nabla_2 & \mathbf{d}^{-1}\\ \nabla_2\mathbf{g}\nabla_2 - \omega^2\boldsymbol{\rho} & \nabla_2\mathbf{h}^\top\end{pmatrix},\quad \begin{gathered}\mathbf{d} = \mathbf{d}_{11},\ \mathbf{h} = -\mathbf{d}_{11}^{-1}\mathbf{d}_{12},\\ \mathbf{g} = \mathbf{d}_{21}\mathbf{d}_{11}^{-1}\mathbf{d}_{12} - \mathbf{d}_{22},\end{gathered}\quad \mathbf{d}_{ij} = \begin{pmatrix}a_{ij} & b_{ji}\\ b_{ij} & c_{ij}\end{pmatrix} = \mathbf{d}_{ji}^\top.\end{gathered} \tag{4}$$

For example if a given piezoelectric material is of cubic point symmetry ($\bar{4}3m$ or 23), then (3) and (4) reduce to

$$\begin{gathered}\mathbf{a} = \mu\mathbf{I},\quad \mathbf{b} = e\mathbf{T},\quad \mathbf{c} = -\varepsilon\mathbf{I};\\ \mathbf{h} = \begin{pmatrix}0 & -e\mu^{-1}\\ e\varepsilon^{-1} & 0\end{pmatrix},\ \mathbf{d} = \begin{pmatrix}\mu & 0\\ 0 & -\varepsilon\end{pmatrix},\ \mathbf{g} = \begin{pmatrix}-\gamma\varepsilon^{-1} & 0\\ 0 & \gamma\mu^{-1}\end{pmatrix},\end{gathered} \tag{5}$$

where $\mu = c_{44} = c_{55}$, $e = e_{14} = e_{25}$, $\varepsilon = \varepsilon_{11} = \varepsilon_{22}$, $\gamma = \mu\varepsilon + e^2$, $\mathbf{I}$ is the 2×2 identity matrix and $\mathbf{T}$ is the 2×2 matrix with zero diagonal and unit off-diagonal entries. For the piezoelectric medium of symmetry ∞m, $6mm$, $4mm$ or $3m$ with the principal axis parallel to X_3, it follows that

$$\mathbf{a} = \mu\mathbf{I},\quad \mathbf{b} = e\mathbf{I},\quad \mathbf{c} = -\varepsilon\mathbf{I};\quad \mathbf{h} = \mathbf{0}_{2\times2},\quad \mathbf{d} = \begin{pmatrix}\mu & e\\ e & -\varepsilon\end{pmatrix} = -\mathbf{g}, \tag{6}$$

where $e = e_{15} = e_{24}$.

3. Spectral asymptotic homogenization method

In this section we present the classical approach of homogenization theory [18] for obtaining effective parameters. The method is essentially just the application of regular perturbation theory to the spectral problem (2) for low frequency ω and small wave number k.

Assume a 2D periodic piezoelectric phononic crystal with a cubic lattice. Applying the quasi-periodic Floquet condition $u = e^{i\mathbf{k}\cdot\mathbf{x}}u_0$, $\varphi = e^{i\mathbf{k}\cdot\mathbf{x}}\varphi_0$ with $\mathbf{k} = k\boldsymbol{\kappa}$, $k = |\mathbf{k}|$ to (1) yields

$$(\mathcal{C}_0 + k\mathcal{C}_1 + k^2\mathcal{C}_2)\mathbf{f} = -\omega^2\boldsymbol{\rho}\mathbf{f} \quad \text{for} \quad \mathbf{f} = \begin{pmatrix} u_0 \\ \varphi_0 \end{pmatrix} \tag{7}$$

where

$$\mathcal{C}_0 = \begin{pmatrix} \boldsymbol{\nabla}^\top\mathbf{a}\boldsymbol{\nabla} & \boldsymbol{\nabla}^\top\mathbf{b}^\top\boldsymbol{\nabla} \\ \boldsymbol{\nabla}^\top\mathbf{b}\boldsymbol{\nabla} & \boldsymbol{\nabla}^\top\mathbf{c}\boldsymbol{\nabla} \end{pmatrix}, \quad \mathcal{C}_2 = -\begin{pmatrix} \boldsymbol{\kappa}^\top\mathbf{a}\boldsymbol{\kappa} & \boldsymbol{\kappa}^\top\mathbf{b}^\top\boldsymbol{\kappa} \\ \boldsymbol{\kappa}^\top\mathbf{b}\boldsymbol{\kappa} & \boldsymbol{\kappa}^\top\mathbf{c}\boldsymbol{\kappa}, \end{pmatrix}, \tag{8}$$

$$\mathcal{C}_1 = i\begin{pmatrix} \boldsymbol{\kappa}^\top\mathbf{a}\boldsymbol{\nabla} & \boldsymbol{\kappa}^\top\mathbf{b}^\top\boldsymbol{\nabla} \\ \boldsymbol{\kappa}^\top\mathbf{b}\boldsymbol{\nabla} & \boldsymbol{\kappa}^\top\mathbf{c}\boldsymbol{\nabla} \end{pmatrix} + i\begin{pmatrix} \boldsymbol{\nabla}^\top\mathbf{a}\boldsymbol{\kappa} & \boldsymbol{\nabla}^\top\mathbf{b}^\top\boldsymbol{\kappa} \\ \boldsymbol{\nabla}^\top\mathbf{b}\boldsymbol{\kappa} & \boldsymbol{\nabla}^\top\mathbf{c}\boldsymbol{\kappa} \end{pmatrix}. \tag{9}$$

Define the effective speed as

$$c = \lim_{k\to 0}\omega(\mathbf{k})/k.$$

Substituting (8), (9) together with

$$\mathbf{f} = \mathbf{f}_0 + k\mathbf{f}_1 + k^2\mathbf{f}_2 + .., \quad \omega^2 = 0 + k\lambda_1 + k^2c^2 + ..$$

into (7) and identifying terms with the same power of k we deduce that

$$\mathbf{f}_0 = \alpha_1\mathbf{f}_{01} + \alpha_2\mathbf{f}_{02} \text{ with } \mathbf{f}_{01} = \begin{pmatrix} 1 \\ 0 \end{pmatrix}, \quad \mathbf{f}_{02} = \begin{pmatrix} 0 \\ 1 \end{pmatrix}; \tag{10}$$

$$\mathbf{f}_1 = -\mathcal{C}_0^{-1}\mathcal{C}_1\mathbf{f}_0, \lambda_1 = 0; \tag{11}$$

$$\mathcal{C}_0\mathbf{f}_2 = -c^2\boldsymbol{\rho}\mathbf{f}_0 + \mathcal{C}_1\mathcal{C}_0^{-1}\mathcal{C}_1\mathbf{f}_0 - \mathcal{C}_2\mathbf{f}_0, \tag{12}$$

where α_1 and α_2 are coefficients to be found. Scalar multiplication of (12) with $\mathbf{f}_{01}$, $\mathbf{f}_{02}$ leads to the equation

$$\begin{pmatrix} \boldsymbol{\kappa}^\top\mathbf{a}_{\text{eff}}\boldsymbol{\kappa} & \boldsymbol{\kappa}^\top\mathbf{b}_{\text{eff}}^\top\boldsymbol{\kappa} \\ \boldsymbol{\kappa}^\top\mathbf{b}_{\text{eff}}\boldsymbol{\kappa} & \boldsymbol{\kappa}^\top\mathbf{c}_{\text{eff}}\boldsymbol{\kappa} \end{pmatrix}\begin{pmatrix} \alpha_1 \\ \alpha_2 \end{pmatrix} = c^2\boldsymbol{\rho}_{\text{eff}}\begin{pmatrix} \alpha_1 \\ \alpha_2 \end{pmatrix} \tag{13}$$

with $\boldsymbol{\rho}_{\text{eff}} = \langle\boldsymbol{\rho}\rangle$ where $\langle\cdot\rangle$ denotes the spatial average, and

$$\boldsymbol{\kappa}^\top\mathbf{a}_{\text{eff}}\boldsymbol{\kappa} = \boldsymbol{\kappa}^\top\langle\mathbf{a}\rangle\boldsymbol{\kappa} + \begin{pmatrix} \boldsymbol{\nabla}^\top\mathbf{a}\boldsymbol{\kappa} \\ \boldsymbol{\nabla}^\top\mathbf{b}\boldsymbol{\kappa} \end{pmatrix}\cdot\mathcal{C}_0^{-1}\begin{pmatrix} \boldsymbol{\nabla}^\top\mathbf{a}\boldsymbol{\kappa} \\ \boldsymbol{\nabla}^\top\mathbf{b}\boldsymbol{\kappa} \end{pmatrix}, \tag{14}$$

$$\boldsymbol{\kappa}^\top\mathbf{b}_{\text{eff}}\boldsymbol{\kappa} = \boldsymbol{\kappa}^\top\langle\mathbf{b}\rangle\boldsymbol{\kappa} + \begin{pmatrix} \boldsymbol{\nabla}^\top\mathbf{b}^\top\boldsymbol{\kappa} \\ \boldsymbol{\nabla}^\top\mathbf{c}\boldsymbol{\kappa} \end{pmatrix}\cdot\mathcal{C}_0^{-1}\begin{pmatrix} \boldsymbol{\nabla}^\top\mathbf{a}\boldsymbol{\kappa} \\ \boldsymbol{\nabla}^\top\mathbf{b}\boldsymbol{\kappa} \end{pmatrix}, \tag{15}$$

$$\boldsymbol{\kappa}^\top\mathbf{c}_{\text{eff}}\boldsymbol{\kappa} = \boldsymbol{\kappa}^\top\langle\mathbf{c}\rangle\boldsymbol{\kappa} + \begin{pmatrix} \boldsymbol{\nabla}^\top\mathbf{b}^\top\boldsymbol{\kappa} \\ \boldsymbol{\nabla}^\top\mathbf{c}\boldsymbol{\kappa} \end{pmatrix}\cdot\mathcal{C}_0^{-1}\begin{pmatrix} \boldsymbol{\nabla}^\top\mathbf{b}^\top\boldsymbol{\kappa} \\ \boldsymbol{\nabla}^\top\mathbf{c}\boldsymbol{\kappa} \end{pmatrix}. \tag{16}$$

According to (13) the effective speed is obtained in the form

$$c^2 = \frac{\boldsymbol{\kappa}^\top\mathbf{a}_{\text{eff}}\boldsymbol{\kappa}}{\langle\rho\rangle} - \frac{\left(\boldsymbol{\kappa}^\top\mathbf{b}_{\text{eff}}\boldsymbol{\kappa}\right)^2}{\langle\rho\rangle\boldsymbol{\kappa}^\top\mathbf{c}_{\text{eff}}\boldsymbol{\kappa}}. \tag{17}$$

Note that there exists another classical approach usually called the asymptotic homogenization method (AHM). This is based on the separation of spatial scales through the introduction of a small parameter,

resulting in effective equations on the "slow" scale, see e.g. [18]. One could make a formal equivalence between the present approach and AMH by identifying the nondimensional fast and slow spatial scales as x and kx; however we have chosen to present the derivations here in terms of regular perturbation methods, which we consider straightforward and transparent. While our representation of effective parameters (14)-(17) is more convenient and compact, the main content is the same as that based on AHM, see e.g. [6], [7]. The presence of the inverse differential operator $\mathcal{C}_0^{-1}$ implies that in order to obtain exact values of the effective parameters we need to solve 2D differential equation with periodic boundary conditions which is equivalent to the corresponding differential equation on the unit cell in the framework of AHM. Except for the special cases (1D, see (26) and (27) in §5) the solution of this equation cannot be expressed in terms of material parameters in an explicit way. Approximate methods for solving differential equations, such as finite elements or variational method or plane-wave expansion (PWE), are applied for numerical calculations. Thus the PWE method (see §6.1) may be seen as the numerical realization of the asymptotic approach via 2D Fourier expansion.

Calculation of the effective constants for a given configuration of material heterogeneity can be used to generate effective properties of corresponding systems. In this regard, rigorous connections between the effective response of different 2D piezoelectric composite systems were established in [19]. These are related to a variety of universal relations, including identities for phase interchange in two component systems, see [14] for a review. A new correspondence relation involving the matrices $\mathbf{a}_{\text{eff}}$, $\mathbf{b}_{\text{eff}}$, $\mathbf{c}_{\text{eff}}$ is noted in the Appendix.

4. MM method

Now we propose a new method of finding effective parameters. In contrast to the classical asymptotic methods where we need to solve 2D differential equation, the new method requires solving a 1D system of differential equations only and consequently has a much smaller numerical error. The main idea of the method is to rewrite the 2D partial differential equation (2) as a 1D differential equation (5) in one coordinate with 1D operator-valued coefficients in another coordinate and then to apply direct integration (multiplicative integral for the monodromy matrix) and perturbation theory. We use a 1D Fourier expansion (see §7) for the operator-valued coefficients and thereby obtain better estimation of the effective speed than by the 2D Fourier expansion (PWE) of the asymptotic-method equations. In principal one can replace 1D Fourier expansion with 1D finite elements or other appropriate numerical techniques.

Let the axes X_1, X_2 be parallel to the in-plane translation vectors of the phononic crystal. The solution of $\boldsymbol{\eta}' = \mathbf{Q}\boldsymbol{\eta}$ in (4) has the following form

$$\boldsymbol{\eta}(x_1) = \mathbf{M}(x_1, 0)\boldsymbol{\eta}_0 \quad \text{with} \quad \mathbf{M}(b, a) = \widehat{\int_a^b} (\mathbf{I} + \mathbf{Q}dx_1),$$

where $\widehat{\int}$ is the multiplicative integral [20]. For brevity we will confine attention to the principal direction $\boldsymbol{\kappa} = \mathbf{e}_1 = (1\ 0)^\top$. With reference to (4), denote

$$\mathbf{Q} = \mathbf{Q}_0 - \omega^2 \mathbf{Q}_1 \quad \text{where} \quad \mathbf{Q}_0 = \begin{pmatrix} \mathbf{h}\nabla_2 & \mathbf{d}^{-1} \\ \nabla_2\mathbf{g}\nabla_2 & \nabla_2\mathbf{h}^\top \end{pmatrix}, \quad \mathbf{Q}_1 = \begin{pmatrix} \mathbf{0} & \mathbf{0} \\ \boldsymbol{\rho} & \mathbf{0} \end{pmatrix}.$$

Introducing

$$\begin{aligned} \mathbf{M}_0(b, a) &= \widehat{\int_a^b} (\mathbf{I} + \mathbf{Q}_0 dx_1), \quad \mathbf{M}_0 \equiv \mathbf{M}_0(1, 0), \\ \mathbf{M}_1 &= \int_0^1 \mathbf{M}_0(1, x)\mathbf{Q}_1(x)\mathbf{M}_0(x, 0)dx, \end{aligned} \tag{18}$$

we have the following low frequency asymptotic expansion of the propagator over one period or the monodromy matrix (MM):

$$\mathbf{M}(1, 0) = \mathbf{M}_0 - \omega^2 \mathbf{M}_1 + \mathrm{O}(\omega^4). \tag{19}$$

Substitute this expansion of $\mathbf{M}$, the expansion of $e^{ik} = 1 + ik + ...$ and

$$\mathbf{w} = \mathbf{w}_0 + k\mathbf{w}_1 + k^2\mathbf{w}_2 + .., \quad \omega^2 = c^2k^2 + ..$$

into the Bloch-Floquet condition

$$\mathbf{M}(1,0)\mathbf{w} = e^{ik}\mathbf{w}.$$

Note that

$$\mathbf{M}_0\mathbf{W}_0 = \mathbf{W}_0, \quad \mathbf{M}_0^*\widetilde{\mathbf{W}}_0 = \widetilde{\mathbf{W}}_0 \quad \text{for} \quad \mathbf{W}_0 = \begin{pmatrix} \mathbf{f}_{01} & \mathbf{f}_{02} \\ \mathbf{0} & \mathbf{0} \end{pmatrix}, \quad \widetilde{\mathbf{W}}_0 = \begin{pmatrix} \mathbf{0} & \mathbf{0} \\ \mathbf{f}_{01} & \mathbf{f}_{02} \end{pmatrix}, \tag{20}$$

where $*$ means Hermitian conjugation, $\mathbf{W}_0$, $\widetilde{\mathbf{W}}_0$ are 4×2 matrices and $\mathbf{f}_{01}$, $\mathbf{f}_{02}$ are defined in (10). Equating the terms with the same power of k then provides the equations

$$\mathbf{w}_0 = \mathbf{W}_0 \begin{pmatrix} \alpha_1 \\ \alpha_2 \end{pmatrix}, \quad \mathbf{w}_1 = i(\mathbf{M}_0 - \mathbf{I})^{-1}\mathbf{w}_0,$$

$$(\mathbf{M}_0 - \mathbf{I})\mathbf{w}_2 = i\mathbf{w}_1 + c^2\mathbf{M}_1\mathbf{w}_0 - \frac{1}{2}\mathbf{w}_0 \tag{21}$$

with the coefficients α_1, α_2 to be found (see eq. (10)). Multiplying (21) by the matrix-function $\widetilde{\mathbf{W}}_0$ we obtain

$$\widetilde{\mathbf{W}}_0^\top(\mathbf{M}_0 - \mathbf{I})^{-1}\mathbf{W}_0 \begin{pmatrix} \alpha_1 \\ \alpha_2 \end{pmatrix} = c^2\boldsymbol{\rho}_{\text{eff}} \begin{pmatrix} \alpha_1 \\ \alpha_2 \end{pmatrix}, \tag{22}$$

which defines the values of the effective quadratic forms (13) for $\boldsymbol{\kappa} = \mathbf{e}_1$. From (22), the effective speed in the direction $\boldsymbol{\kappa} = \mathbf{e}_1$ follows as

$$c^2(\mathbf{e}_1) = \frac{m_1}{\langle\rho\rangle} - \frac{m_2^2}{\langle\rho\rangle m_4}, \tag{23}$$

where

$$\begin{pmatrix} m_1 & m_2 \\ m_3 & m_4 \end{pmatrix} \equiv \widetilde{\mathbf{W}}_0^\top(\mathbf{M}_0 - \mathbf{I})^{-1}\mathbf{W}_0. \tag{24}$$

The equality $m_2 = m_3$ can be shown using $\mathbf{M}_0^+ = \mathbf{T}\mathbf{M}_0^{-1}\mathbf{T}^{-1}$ and (20). Note that the inverse in eq. (24) is to be considered in the sense of the generalized or pseudo-inverse matrix. This feature is evident in a simple although illustrative application of eq. (23) given in the next section. The general implementation of eq. (24) is discussed in §6.

5. 1D-periodicity case

5.1. General solution

Consider the case of 1D-periodicity, i.e. suppose that all material properties depend periodically on x_1 and do not depend on x_2. This case is known to admit explicit formulas for effective parameters. They can be obtained from (14)-(16) with ∇_2 omitted so that

$$\mathcal{C}_0 = \nabla_1\mathbf{d}_{11}\nabla_1, \quad \begin{pmatrix} \boldsymbol{\nabla}^\top\mathbf{a}\boldsymbol{\kappa} \\ \boldsymbol{\nabla}^\top\mathbf{b}\boldsymbol{\kappa} \end{pmatrix} = \nabla_1\mathbf{d}_3\boldsymbol{\kappa}, \quad \begin{pmatrix} \boldsymbol{\nabla}^\top\mathbf{b}\boldsymbol{\kappa} \\ \boldsymbol{\nabla}^\top\mathbf{c}\boldsymbol{\kappa} \end{pmatrix} = \nabla_1\mathbf{d}_4\boldsymbol{\kappa},$$

where

$$\mathbf{d}_1 = \begin{pmatrix} a_{11} & a_{12} \\ b_{11} & b_{12} \end{pmatrix}, \quad \mathbf{d}_2 = \begin{pmatrix} b_{11} & b_{12} \\ c_{11} & c_{12} \end{pmatrix}.$$

Then

$$\begin{aligned} \mathbf{a}_{\text{eff}} &= \langle\mathbf{a}\rangle - \langle\mathbf{d}_1^\top\mathbf{d}^{-1}\mathbf{d}_1\rangle + \langle\mathbf{d}_1^\top\mathbf{d}^{-1}\rangle\langle\mathbf{d}^{-1}\rangle^{-1}\langle\mathbf{d}^{-1}\mathbf{d}_1\rangle, \\ \boldsymbol{\kappa}^\top\mathbf{b}_{\text{eff}}\boldsymbol{\kappa} &= \boldsymbol{\kappa}^\top(\langle\mathbf{b}\rangle - \langle\mathbf{d}_2^\top\mathbf{d}^{-1}\mathbf{d}_1\rangle + \langle\mathbf{d}_2^\top\mathbf{d}^{-1}\rangle\langle\mathbf{d}^{-1}\rangle^{-1}\langle\mathbf{d}^{-1}\mathbf{d}_1\rangle)\boldsymbol{\kappa}, \\ \mathbf{c}_{\text{eff}} &= \langle\mathbf{c}\rangle - \langle\mathbf{d}_2^\top\mathbf{d}^{-1}\mathbf{d}_2\rangle + \langle\mathbf{d}_2^\top\mathbf{d}^{-1}\rangle\langle\mathbf{d}^{-1}\rangle^{-1}\langle\mathbf{d}^{-1}\mathbf{d}_2\rangle, \end{aligned} \tag{25}$$

where now $\langle\cdot\rangle = \int_0^1 \cdot\, dx_1$ and it has been taken into account that $\mathbf{a}_{\text{eff}}$, $\mathbf{c}_{\text{eff}}$ are self-adjoint (real symmetric) matrices, while $\mathbf{b}_{\text{eff}}$ is generally not and hence its quadratic form defines $\mathbf{b}_{\text{eff}}$ up to an arbitrary skew-symmetric matrix. The above results for the 1D case also follow from the equality $\mathbf{Q}_{\text{eff}} = \langle \mathbf{Q} \rangle$, see [21], [14, Section 9.5]. Note that the 1D case is an exception in that the different methods provide the same (exact) effective coefficients.

For example, applying (25) to the cases (5) and (6) yields, respectively,

$$\begin{aligned}
\mathbf{a}_{\text{eff}} &= \begin{pmatrix} \langle \mu^{-1} \rangle^{-1} & 0 \\ 0 & \langle \gamma\varepsilon^{-1} \rangle - \langle e\varepsilon^{-1} \rangle^2 \langle \varepsilon^{-1} \rangle^{-1} \end{pmatrix}, \\
\mathbf{b}_{\text{eff}} &= \frac{1}{2}\big(\langle e\varepsilon^{-1} \rangle \langle \varepsilon^{-1} \rangle^{-1} + \langle e\mu^{-1} \rangle \langle \mu^{-1} \rangle^{-1} \big) \begin{pmatrix} 0 & 1 \\ 1 & 0 \end{pmatrix}, \\
\mathbf{c}_{\text{eff}} &= \begin{pmatrix} -\langle \varepsilon^{-1} \rangle^{-1} & 0 \\ 0 & -\langle \gamma\mu^{-1} \rangle + \langle e\mu^{-1} \rangle^2 \langle \mu^{-1} \rangle^{-1} \end{pmatrix},
\end{aligned} \tag{26}$$

and

$$\mathbf{a}_{\text{eff}} = \begin{pmatrix} \left\langle \mu\gamma^{-1} \right\rangle \Gamma^{-1} & 0 \\ 0 & \langle \mu \rangle \end{pmatrix}, \quad \mathbf{b}_{\text{eff}} = \begin{pmatrix} \left\langle e\gamma^{-1} \right\rangle \Gamma^{-1} & 0 \\ 0 & \langle e \rangle \end{pmatrix}, \quad \mathbf{c}_{\text{eff}} = \begin{pmatrix} -\left\langle \varepsilon\gamma^{-1} \right\rangle \Gamma^{-1} & 0 \\ 0 & -\langle \varepsilon \rangle \end{pmatrix}, \tag{27}$$

where $\Gamma = \left\langle \mu\gamma^{-1} \right\rangle \left\langle \varepsilon\gamma^{-1} \right\rangle + \left\langle e\gamma^{-1} \right\rangle^2$ and it is assumed that $\mathbf{b}_{\text{eff}}$ is symmetric, as was the original $\mathbf{b}$ in (5) and (6).

5.2. Effective wave speed using MM method

It is instructive to see how the MM method applies to the 1D-periodic medium. Based upon its definition in (18) and the 1D structure, it follows that $\mathbf{M}_0(1,0) = \mathbf{I} + \langle \mathbf{Q}_0 \rangle$. The MM result (24) then becomes

$$\begin{aligned}
\begin{pmatrix} m_1 & m_2 \\ m_3 & m_4 \end{pmatrix} &= \widetilde{\mathbf{W}}_0^{\top} \begin{pmatrix} \mathbf{0} & \langle \mathbf{d}^{-1} \rangle \\ \mathbf{0} & \mathbf{0} \end{pmatrix}^{-1} \mathbf{W}_0 \\
&= \langle \mathbf{d}^{-1} \rangle^{-1}
\end{aligned}$$

which yields the correct effective wave speed using (23).

6. Implementation

6.1. PWE method

Let us denote the 2D Fourier coefficients for any $\mathbf{1}$-periodic function $r(\mathbf{x})$ as $\hat{r}(\mathbf{g})$, i.e.

$$r(\mathbf{x}) = \sum_{\mathbf{g} \in \mathbb{Z}^2} \hat{r}(\mathbf{g}) e^{2\pi i \mathbf{g}\cdot\mathbf{x}}, \quad \hat{r}(\mathbf{g}) = \int\limits_{[0,1]^2} e^{-2\pi i \mathbf{g}\cdot\mathbf{x}} r(\mathbf{x}) d\mathbf{x}. \tag{28}$$

We can therefore rewrite (14)–(16) in terms of the Fourier coefficients as

$$\boldsymbol{\kappa}^{\top} \mathbf{a}_{\text{eff}} \boldsymbol{\kappa} = \boldsymbol{\kappa}^{\top} \langle \mathbf{a} \rangle \boldsymbol{\kappa} - \begin{pmatrix} \hat{a}_{ij}(\mathbf{g}) g_i \kappa_j \\ \hat{b}_{ij}(\mathbf{g}) g_i \kappa_j \end{pmatrix}^{*} \mathbf{C}_0^{-1} \begin{pmatrix} \hat{a}_{ij}(\mathbf{g}) g_i \kappa_j \\ \hat{b}_{ij}(\mathbf{g}) g_i \kappa_j \end{pmatrix}, \tag{29}$$

$$\boldsymbol{\kappa}^{\top} \mathbf{b}_{\text{eff}} \boldsymbol{\kappa} = \boldsymbol{\kappa}^{\top} \langle \mathbf{b} \rangle \boldsymbol{\kappa} - \begin{pmatrix} \hat{b}_{ji}(\mathbf{g}) g_i \kappa_j \\ \hat{c}_{ij}(\mathbf{g}) g_i \kappa_j \end{pmatrix}^{*} \mathbf{C}_0^{-1} \begin{pmatrix} \hat{a}_{ij}(\mathbf{g}) g_i \kappa_j \\ \hat{b}_{ij}(\mathbf{g}) g_i \kappa_j \end{pmatrix}, \tag{30}$$

$$\boldsymbol{\kappa}^{\top} \mathbf{c}_{\text{eff}} \boldsymbol{\kappa} = \boldsymbol{\kappa}^{\top} \langle \mathbf{c} \rangle \boldsymbol{\kappa} - \begin{pmatrix} \hat{b}_{ji}(\mathbf{g}) g_i \kappa_j \\ \hat{c}_{ij}(\mathbf{g}) g_i \kappa_j \end{pmatrix}^{*} \mathbf{C}_0^{-1} \begin{pmatrix} \hat{b}_{ji}(\mathbf{g}) g_i \kappa_j \\ \hat{c}_{ij}(\mathbf{g}) g_i \kappa_j \end{pmatrix}, \tag{31}$$

where

$$\mathbf{C}_0 \equiv \begin{pmatrix} \hat{a}_{ij}(\mathbf{g} - \mathbf{g}') g_i g'_j & \hat{b}_{ji}(\mathbf{g} - \mathbf{g}') g_i g'_j \\ \hat{b}_{ij}(\mathbf{g} - \mathbf{g}') g_i g'_j & \hat{c}_{ij}(\mathbf{g} - \mathbf{g}') g_i g'_j \end{pmatrix} \tag{32}$$

and $\mathbf{g}, \mathbf{g}'$ belong to the set $\mathbb{Z}^2 \setminus \mathbf{0}$. For practical use all matrices are assumed to be of finite size $2(2N+1)^2 \times 2(2N+1)^2$, where N is a number of Fourier harmonics in one coordinate.

6.2. MM method

In this case we need only Fourier coefficients in x_2. Denote it as $\hat{a}_n(x_1)$ for any x_2-periodic function $a(x_1, x_2)$, i.e.

$$a(x_1, x_2) = \sum_{n\in\mathbb{Z}} \hat{a}_n(x_1) e^{2\pi i n x_2}, \quad \hat{a}_n(x_1) = \int_0^1 e^{-2\pi i n x_2} a(x_1, x_2) dx_2. \tag{33}$$

We can now rewrite the operators (4) in terms of Fourier coefficients as follows

$$\hat{\mathbf{d}}_{ij}(x_1) \equiv \begin{pmatrix} (\hat{a}_{ij})_{n-m}(x_1) & (\hat{b}_{ji})_{n-m}(x_1) \\ (\hat{b}_{ij})_{n-m}(x_1) & (\hat{c}_{ij})_{n-m}(x_1) \end{pmatrix}, \quad n, m \in \mathbb{Z}, \tag{34}$$

$$\hat{\mathbf{d}} \equiv \hat{\mathbf{d}}_{11}, \quad \hat{\mathbf{h}} \equiv -\hat{\mathbf{d}}_{11}^{-1}\hat{\mathbf{d}}_{12}, \quad \hat{\mathbf{g}} \equiv \hat{\mathbf{d}}_{21}\hat{\mathbf{d}}_{11}^{-1}\hat{\mathbf{d}}_{12} - \hat{\mathbf{d}}_{22}, \tag{35}$$

$$\hat{\boldsymbol{\nabla}} \equiv 2\pi i \begin{pmatrix} \mathrm{diag}(n) & \mathbf{0} \\ \mathbf{0} & \mathrm{diag}(n) \end{pmatrix}, \quad \hat{\mathbf{Q}}_0 \equiv \begin{pmatrix} \hat{\mathbf{h}}\hat{\boldsymbol{\nabla}} & \hat{\mathbf{d}}^{-1} \\ \hat{\boldsymbol{\nabla}}\hat{\mathbf{g}}\hat{\boldsymbol{\nabla}} & \hat{\boldsymbol{\nabla}}\hat{\mathbf{h}}^* \end{pmatrix}. \tag{36}$$

For practical use the matrix $\hat{\mathbf{Q}}_0$ is assumed to be of finite size $4(2N+1) \times 4(2N+1)$, where N is the number of Fourier harmonics in the x_2-coordinate. To find the effective matrix (24) we need to calculate the monodromy matrix $\hat{\mathbf{M}}_0 = \widehat{\int_0^1}(\mathbf{I} + \hat{\mathbf{Q}}_0 dx_1)$. But this is not an effective approach because the components of $\hat{\mathbf{M}}_0$ grow exponentially. It is better to use the resolvent $\hat{\mathbf{R}}_0 = (\hat{\mathbf{M}}_0 - \alpha\mathbf{I})^{-1}$ whose components have moderate growth. We cannot take $\alpha = 1$ as required in (24) because $(\mathbf{M}_0 - \mathbf{I})^{-1}$ does not exist (1 is eigenvalue of $\mathbf{M}_0$, see (20)), only the inverse image $(\mathbf{M}_0 - \mathbf{I})^{-1}\mathbf{W}_0$ exists. Generally we need to take α beyond the spectrum of $\hat{\mathbf{M}}_0$. Recall that $\hat{\mathbf{M}}_0$ satisfies $\hat{\mathbf{M}}_0' = \hat{\mathbf{Q}}_0\hat{\mathbf{M}}_0$ and $\hat{\mathbf{M}}(0) = \mathbf{I}$, which implies that the resolvent $\hat{\mathbf{R}}(x_1) = (\hat{\mathbf{M}}_0(x_1) - \alpha\mathbf{I})^{-1}$ satisfies

$$\begin{cases} \hat{\mathbf{R}}' = -\hat{\mathbf{R}}\hat{\mathbf{Q}}_0(\mathbf{I} + \alpha\hat{\mathbf{R}}), \\ \hat{\mathbf{R}}(0) = (1-\alpha)^{-1}\mathbf{I}. \end{cases} \tag{37}$$

So we can take some complex α far enough from the real axis and the unit circle and solve the differential system (37) to find $\hat{\mathbf{R}}_0 \equiv \hat{\mathbf{R}}(1)$. Note the identity

$$\begin{aligned} (\mathbf{M}_0 - \mathbf{I})^{-1}\mathbf{W}_0 &= (\mathbf{I} - (1-\alpha)\mathbf{R}_0)^{-1}\mathbf{R}_0\mathbf{W}_0 \\ &= (\mathbf{I} - (1-\alpha)\mathbf{R}_0)^{-1}\frac{\mathbf{W}_0}{1-\alpha} \end{aligned} \tag{38}$$

with $\mathbf{R}_0 = (\mathbf{M}_0 - \alpha\mathbf{I})^{-1}$. Then the effective matrix (24) is

$$\begin{pmatrix} m_1 & m_2 \\ m_3 & m_4 \end{pmatrix} = \frac{1}{1-\alpha}\widehat{\widetilde{\mathbf{W}}}_0^*(\mathbf{I} - (1-\alpha)\hat{\mathbf{R}}_0)^{-1}\widehat{\mathbf{W}}_0, \tag{39}$$

where the Fourier transforms of $\widetilde{\mathbf{W}}$ and $\mathbf{W}$ are

$$\widehat{\widetilde{\mathbf{W}}}_0 = \begin{pmatrix} \mathbf{0} & \mathbf{0} \\ \mathbf{0} & \mathbf{0} \\ \delta_{n0} & \mathbf{0} \\ \mathbf{0} & \delta_{n0} \end{pmatrix}, \quad \widehat{\mathbf{W}}_0 = \begin{pmatrix} \delta_{n0} & \mathbf{0} \\ \mathbf{0} & \delta_{n0} \\ \mathbf{0} & \mathbf{0} \\ \mathbf{0} & \mathbf{0} \end{pmatrix}, \quad n \in \mathbb{Z}. \tag{40}$$

Note that there is no inverse matrix of $(\mathbf{I} - (1-\alpha)\hat{\mathbf{R}}_0)$ in (39), because it has two zero rows and columns. Nevertheless, the inverse image $(\mathbf{I} - (1-\alpha)\hat{\mathbf{R}}_0)^{-1}\hat{\mathbf{W}}_0$ exists (although not unique) and the effective matrix (m_i) is uniquely defined.

7. Examples

We plot the dependence of effective speed on the filling fraction of square or circular cross-sectional inclusions in a two-component 2D phononic crystal where the piezoelectric fraction is either the inclusion or the matrix, see Figs. 1-3. The material parameters are $\mu = 1.482$ GPa, $\rho = 1.142$ g/cm^3 for Epoxy; $\mu = 60$ GPa, $e = 3.7$ C/m^2, $\varepsilon = 0.389$ nF/m, $\rho = 4.7$ g/cm^3 for $LiNbO_3$, and $\mu = 25.6$ GPa, $e = 12.7$ C/m^2, $\varepsilon = 0.65$ nF/m, $\rho = 7.5$ g/cm^3 for ceramic CTS-4. Figures 1-3 (a,b) show the results obtained by the PWE and MM methods. It is seen that, for a given value of N, the number of Fourier harmonics used, the MM formula (23) with (39), (40) is more accurate than the PWE formula (17) with (29)-(32). The convergence of the MM curves is uniformly faster than that of the PWE curves, especially in the case of densely packed stiff inclusions in a soft matrix. The latter observation coincides with the same feature established for pure elastic phononic crystals, see [17]. it is not surprising that the MM converges faster considering that it requires only N Fourier harmonics in the lateral directions as compared with N^2 for the PWE method (and even larger matrices of size $2(2N+1)^2 \times 2(2N+1)^2$). However, the accuracy of the MM method for very small values of N (even $N = 0$) is quite unexpected and surprising. Note that the MM-method with $N = 0$ provides a closed-form approximation of the effective speed

$$c_0^2(\mathbf{e}_1) = \frac{1}{\langle \rho \rangle} \det \left\langle \begin{pmatrix} \langle a_{11} \rangle_2 & \langle b_{11} \rangle_2 \\ \langle b_{11} \rangle_2 & \langle c_{11} \rangle_2 \end{pmatrix}^{-1} \right\rangle_1^{-1} \tag{41}$$

where $\langle \cdot \rangle_j = \int_0^1 \cdot \, dx_j$. Figures 1-3 (c,d) compare the results obtained by the MM method with and without accounting for the piezoelectricity.

8. Conclusions

The PWE and MM methods of calculating quasistatic effective SH wave speeds in two-dimensional piezoelectric phononic crystals have been formulated and compared. Explicit expression for the effective quasistatic wave speed are given by eq. (17) for the PWE method and by eq. (23) for the new MM approach. The MM method can be viewed as a one-dimensional PWE combined with a one-dimensional differential equation which is solved numerically to yield the monodromy matrix. The examples of §7 show that the MM method provides more accurate approximations than the PWE scheme, consistent with previous comparisons for 2D and 3D elastic PCs [16, 17]. The numerical results also indicate that when calculating effective speeds in phononic crystals with piezoelectric inclusion or/and matrix, it is necessary to take into account piezoelectric properties, especially if they are strong enough (compare Figs. 1-3 (c,d)).

Appendix: Correspondence relations between effective properties of different systems

Denote the connection between the initial and effective properties by (see eq. (4))

$$\begin{pmatrix} \mathbf{d}_{11} & \mathbf{d}_{12} \\ \mathbf{d}_{21} & \mathbf{d}_{22} \end{pmatrix} \mapsto \begin{pmatrix} \mathbf{d}_{11}^{\text{eff}} & \mathbf{d}_{12}^{\text{eff}} \\ \mathbf{d}_{21}^{\text{eff}} & \mathbf{d}_{22}^{\text{eff}} \end{pmatrix}. \tag{42}$$

Consider a composite with properties

$$\begin{pmatrix} \tilde{\mathbf{d}}_{11} & \tilde{\mathbf{d}}_{12} \\ \tilde{\mathbf{d}}_{21} & \tilde{\mathbf{d}}_{22} \end{pmatrix} = \begin{pmatrix} \mathbf{d}_{22} & -\mathbf{d}_{21} \\ -\mathbf{d}_{12} & \mathbf{d}_{11} \end{pmatrix}^{-1} \tag{43}$$

then it can be shown that its effective properties satisfy [19, Eq. (33)]

$$\begin{pmatrix} \tilde{\mathbf{d}}_{11}^{\text{eff}} & \tilde{\mathbf{d}}_{12}^{\text{eff}} \\ \tilde{\mathbf{d}}_{21}^{\text{eff}} & \tilde{\mathbf{d}}_{22}^{\text{eff}} \end{pmatrix} = \begin{pmatrix} \mathbf{d}_{22}^{\text{eff}} & -\mathbf{d}_{21}^{\text{eff}} \\ -\mathbf{d}_{12}^{\text{eff}} & \mathbf{d}_{11}^{\text{eff}} \end{pmatrix}^{-1}. \tag{44}$$

We also present a similar relation in terms of other matrices, specifically

$$\begin{pmatrix} \mathbf{a} & \mathbf{b}^\top \\ \mathbf{b} & \mathbf{c} \end{pmatrix} \mapsto \begin{pmatrix} \mathbf{a}_{\text{eff}} & \mathbf{b}_{\text{eff}}^\top \\ \mathbf{b}_{\text{eff}} & \mathbf{c}_{\text{eff}} \end{pmatrix}. \tag{45}$$

Consider the initial matrix of the form of

$$\begin{pmatrix} \tilde{\mathbf{a}}(\mathbf{x}) & \tilde{\mathbf{b}}^\top(\mathbf{x}) \\ \tilde{\mathbf{b}}(\mathbf{x}) & \tilde{\mathbf{c}}(\mathbf{x}) \end{pmatrix} := \begin{pmatrix} \mathbf{a}(\boldsymbol{\sigma}\mathbf{x}) & \mathbf{b}^\top(\boldsymbol{\sigma}\mathbf{x}) \\ \mathbf{b}(\boldsymbol{\sigma}\mathbf{x}) & \mathbf{c}(\boldsymbol{\sigma}\mathbf{x}) \end{pmatrix}^{-1} \text{ with rotation } \boldsymbol{\sigma} = \begin{pmatrix} 0 & 1 \\ -1 & 0 \end{pmatrix}. \tag{46}$$

The corresponding effective matrix we denote as

$$\begin{pmatrix} \tilde{\mathbf{a}} & \tilde{\mathbf{b}}^\top \\ \tilde{\mathbf{b}} & \tilde{\mathbf{c}} \end{pmatrix} \mapsto \begin{pmatrix} \tilde{\mathbf{a}}_{\text{eff}} & \tilde{\mathbf{b}}_{\text{eff}}^\top \\ \tilde{\mathbf{b}}_{\text{eff}} & \tilde{\mathbf{c}}_{\text{eff}} \end{pmatrix}. \tag{47}$$

By analogy with the elastic case (see [18]) it can be proved that

$$\begin{pmatrix} \tilde{\mathbf{a}}_{\text{eff}} & \tilde{\mathbf{b}}_{\text{eff}}^\top \\ \tilde{\mathbf{b}}_{\text{eff}} & \tilde{\mathbf{c}}_{\text{eff}} \end{pmatrix} = \begin{pmatrix} \mathbf{a}_{\text{eff}} & \mathbf{b}_{\text{eff}}^\top \\ \mathbf{b}_{\text{eff}} & \mathbf{c}_{\text{eff}} \end{pmatrix}^{-1}. \tag{48}$$

Acknowledgement. This work has been conducted in the framework of the project MIRAGES ANR-12-BS09-0015 with the support of the Competitiveness Cluster Aerospace Valley. ANN is grateful for support from the Fulbright U.S. Scholar Program.

[1] A.A. Grekov, S.O Kramarov, and A.A. Kuprienko. Effectective properties of a transversely isotropic piezocomposite with cylindrical inclusions. *Ferroelectrics*, 99:11526, 1989.
[2] M. Dunn and M. Taya. Micromechanics predictions of the effective electroelastic moduli of piezoelectric composites. *Int. J. Engng. Sc.*, 30:16175, 1993.
[3] P. Tan and L. Tong. Micro-electromechanics models for piezoelectric-fiber-reinforced composite materials. *Comp. Science Tech.*, 61(5):759 – 769, 2001.
[4] N. Turbé and G. A. Maugin. On the linear piezoelectricity of composite materials. *Math. Meth. Appl. Sci.*, 14(6):403–412, 1991.
[5] R. Guinovart-Díaz, P. Yan, R. Rodríguez-Ramos, J. C. López-Realpozo, C. P. Jiang, J. Bravo-Castillero, and F. J. Sabina. Effective properties of piezoelectric composites with parallelogram periodic cells. *Int. J. Engng. Sc.*, 53:58–66, 2012.
[6] F. J. Sabina, R. Rodrıguez-Ramos, J. Bravo-Castillero, and R. Guinovart-Dıaz. Closed-form expressions for the effective coefficients of a fibre-reinforced composite with transversely isotropic constituents. II: Piezoelectric and hexagonal symmetry. *J. Mech. Phys. Solids*, 49(7):1463–1479, 2001.
[7] P. Yan, C. P. Jiang, and F. Song. An eigenfunction expansion-variational method for the anti-plane electroelastic behavior of three-phase fiber composites. *Mech. Mater.*, 43(10):586–597, 2011.
[8] H. Berger, S. Kari, U. Gabbert, R. Rodriguez-Ramos, J. Bravo-Castillero, R. Guinovart-Diaz, F. J. Sabina, and G. A. Maugin. Unit cell models of piezoelectric fiber composites for numerical and analytical calculation of effective properties. *Smart Mater. Struct.*, 15(2):451–458, 2006.
[9] E. Lenglet, A-C Hladky-Hennion, and J-C Debus. Numerical homogenization techniques applied to piezoelectric composites. *J. Acoust. Soc. Am.*, 113(2):826–833, 2003.
[10] E. López-López, F. J. Sabina, J. Bravo-Castillero, R. Guinovart-Díaz, and R. Rodríguez-Ramos. Overall electromechanical properties of a binary composite with 622 symmetry constituents. *Int. J. Solids Struct.*, 42(21-22):5765–5777, 2005.
[11] Y. L. Xu, S. H. Lo, C. P. Jiang, and Y. K. Cheung. Electroelastic behavior of doubly periodic piezoelectric fiber composites under antiplane shear. *Int. J. Solids Struct.*, 44(3-4):976–995, 2007.
[12] N. Rylko. Effective anti-plane properties of piezoelectric fibrous composites. *Acta Mech.*, online, 2013.
[13] B. Wang. Effective behavior of piezoelectric composites. *Appl. Mech. Rev.*, 47:S112–121, 1994.
[14] G. W. Milton. *The Theory of Composites*. Cambridge University Press, 1st edition, 2001.
[15] A. A. Krokhin, J. Arriaga, and L. N. Gumen. Speed of sound in periodic elastic composites. *Phys. Rev. Lett.*, 91(26):264302+, 2003.
[16] A. A. Kutsenko, A. L. Shuvalov, A. N. Norris, and O. Poncelet. On the effective shear speed in 2D phononic crystals. *Phys. Rev. B*, 84:064305, 2011.
[17] A. A. Kutsenko, A. L. Shuvalov, and A. N. Norris. On the quasistatic effective elastic moduli for elastic waves in three-dimensional phononic crystals. *J. Mech. Phys. Solids*, 61(11):2260-2272, 2013.
[18] V. V. Jikov, S. M. Kozlov, and O. A. Oleĭnik. *Homogenization of Differential Operators and Integral Functionals*. Berlin: Springer-Verlag, 1994. Translated from the Russian by G. A. Yosifian.
[19] Y. Benveniste. Correspondence relations among equivalent classes of heterogeneous piezoelectric solids under anti-plane mechanical and in-plane electrical fields. *J. Mech. Phys. Solids*, 43(4):553–571, 1995.
[20] M. C. Pease. *Methods of Matrix Algebra*. Academic Press, New York, 1965.
[21] S.M. Kikkarin and D.V. Petrov. Effective elastic, piezoelectric and dielectric constants of superlattices. *Kristallografiya*, 34:1072–1075, 1989, in Russian.

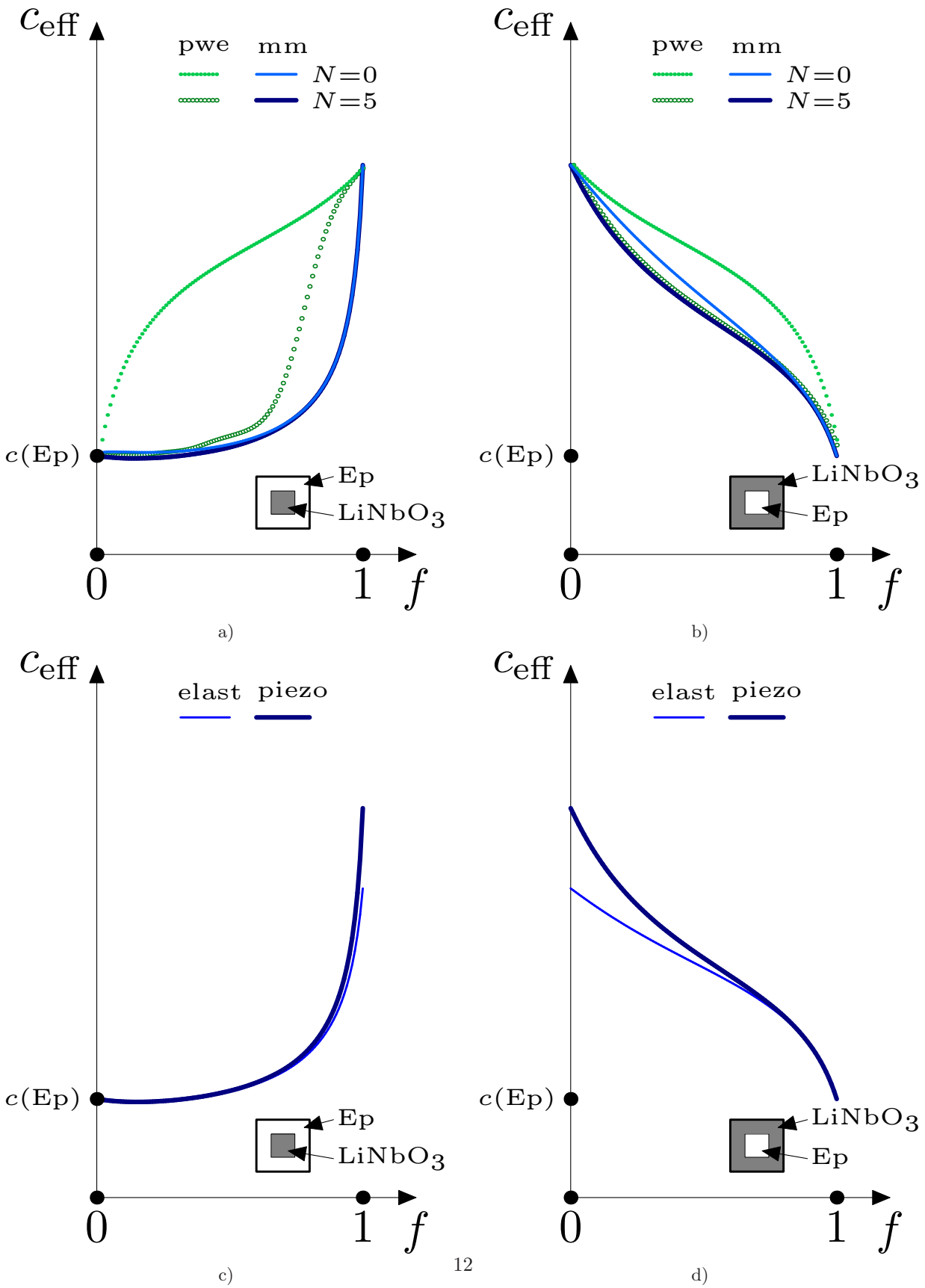

Figure 1: The SH effective speed in the matrix/inclusion = epoxy/$LiNbO_3$ and $LiNbO_3$/epoxy phononic crystals versus filing fraction f of the inclusion. (a,b) PWE and MM estimates calculated with $N = 0$ and $N = 5$ Fourier harmonics. (c,d) MM estimate calculated with $N = 10$ with and without account for piezoelectric effect.

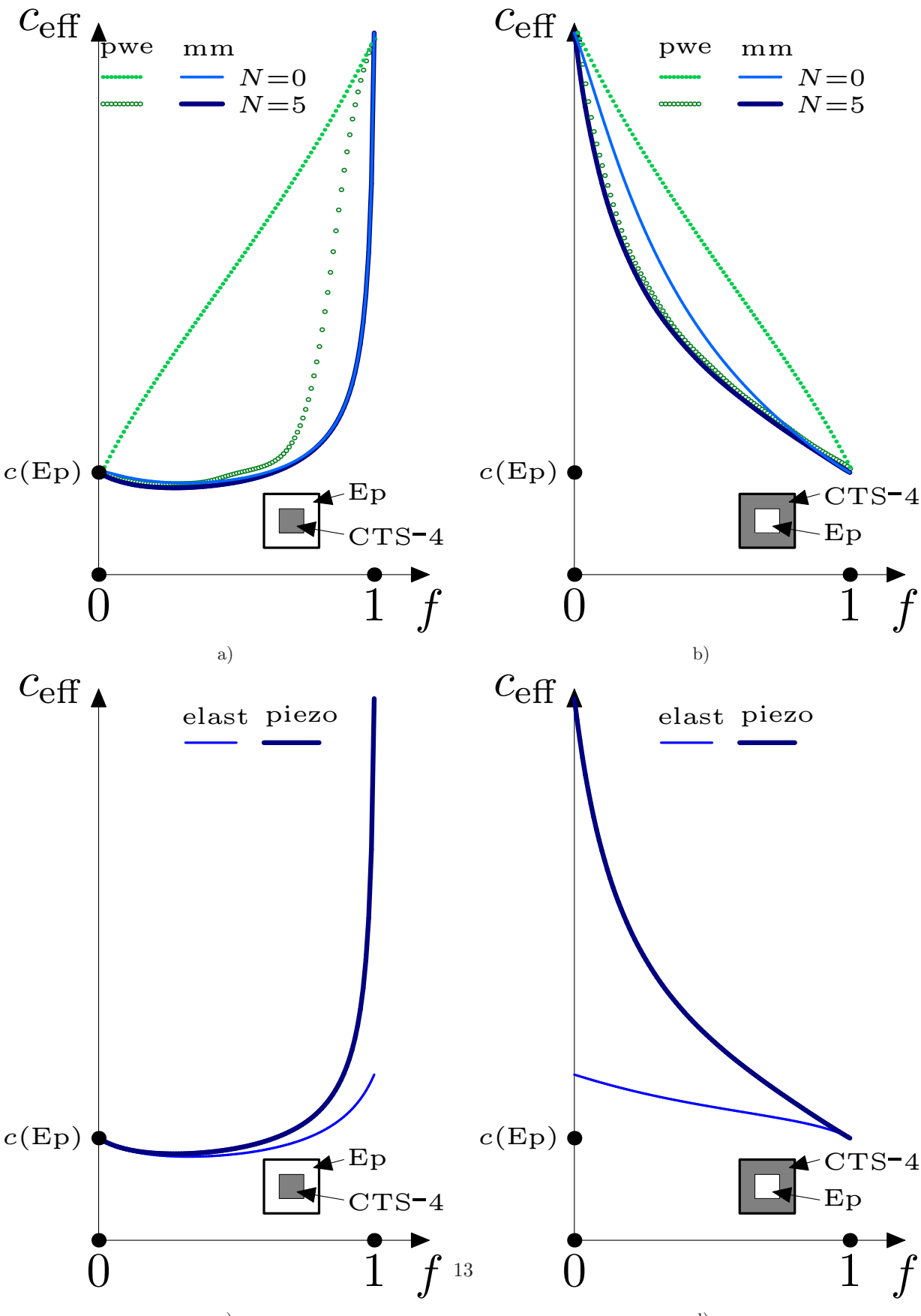

Figure 2: The same as in Fig. 1 with CTS-4 instead of $LiNbO_3$.

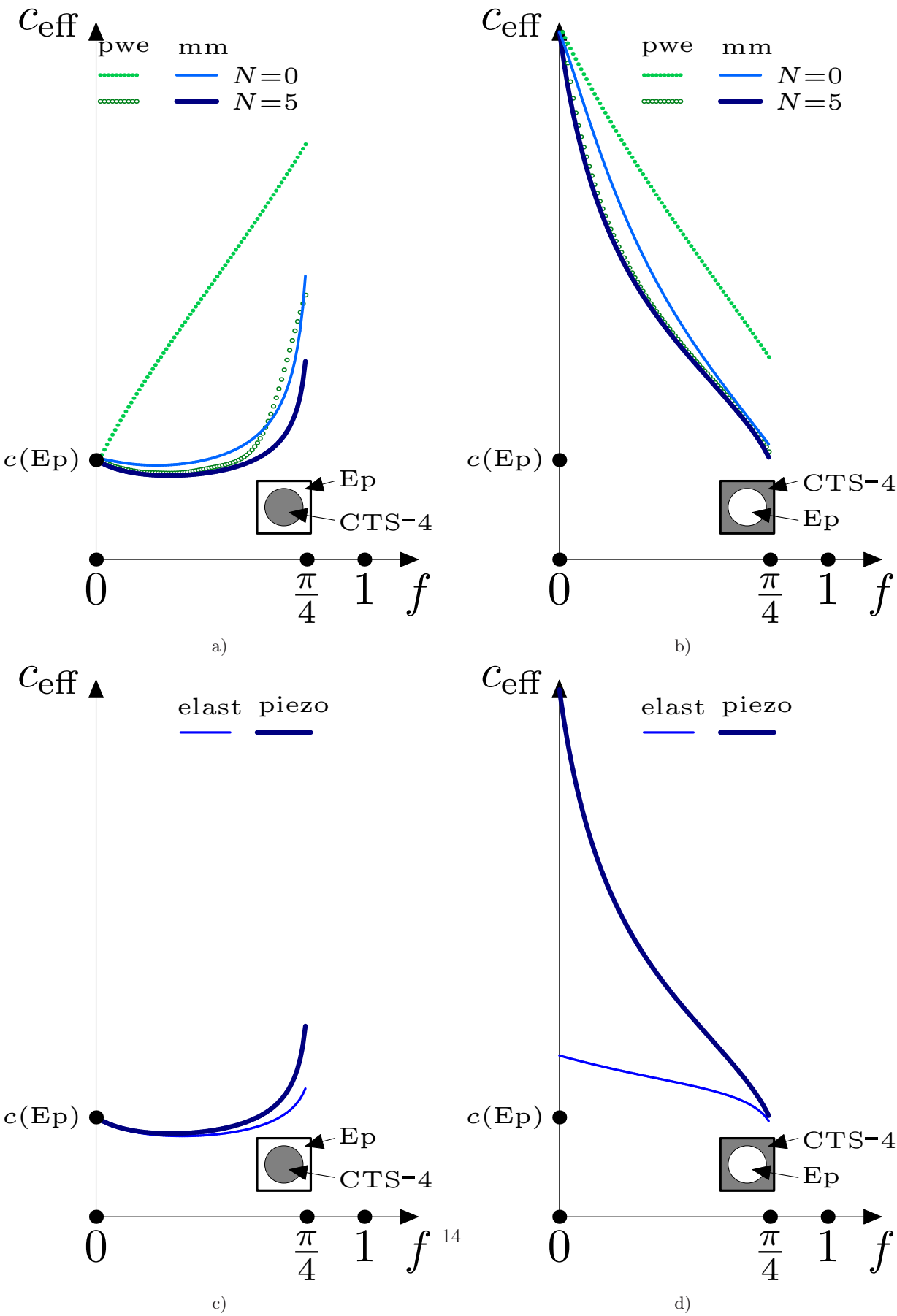

Figure 3: The same as in Fig. 2 with circular instead of square inclusions.